Airway in Color

Yuanhong Sun

Confocal fluorescence imaging of differentiated human airway epithelial cells cultured at an air–liquid interface. Basal (KRT5), ciliated (tubulin I/II), and goblet (MUC5AC, TFF3) cell populations are distinctly visualized, with ZO-1 outlining intact tight junctions. Nuclei are labeled with DAPI. Maximum-projection and orthogonal views highlight the layered architecture and successful mucociliary differentiation of the ALI model. Scale bar: 20 μm.

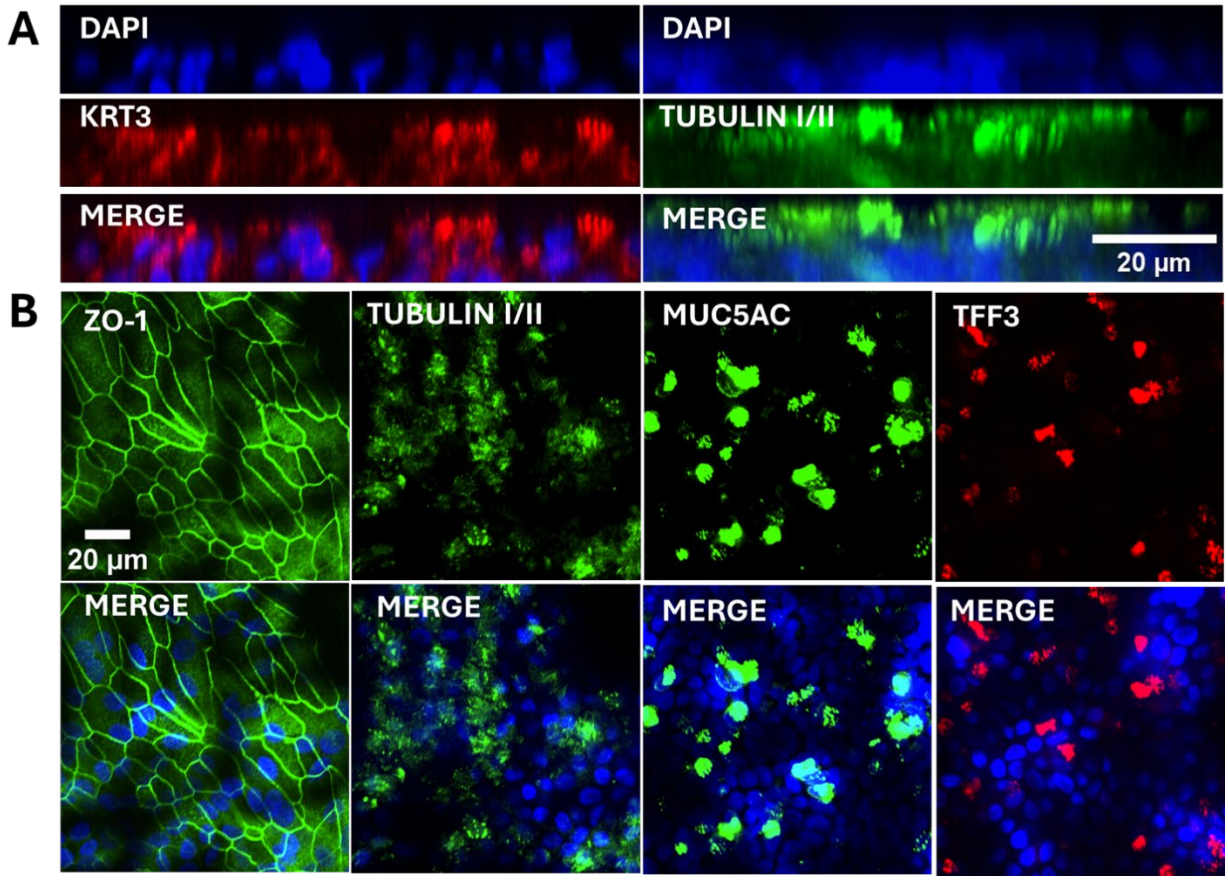

Love triangle

Rudy Villa

SEM micrograph of deformation bands inside of a pore found on the fracture surface of a CoCrMo alloy material that was tensile tested. Bulk sample deformation caused metal flow inside a pore cavity that resulted in the activation of the (111) slip system in the FCC matrix. Nodular features are carbides that also formed along the grain boundary observed at the bottom of the image.

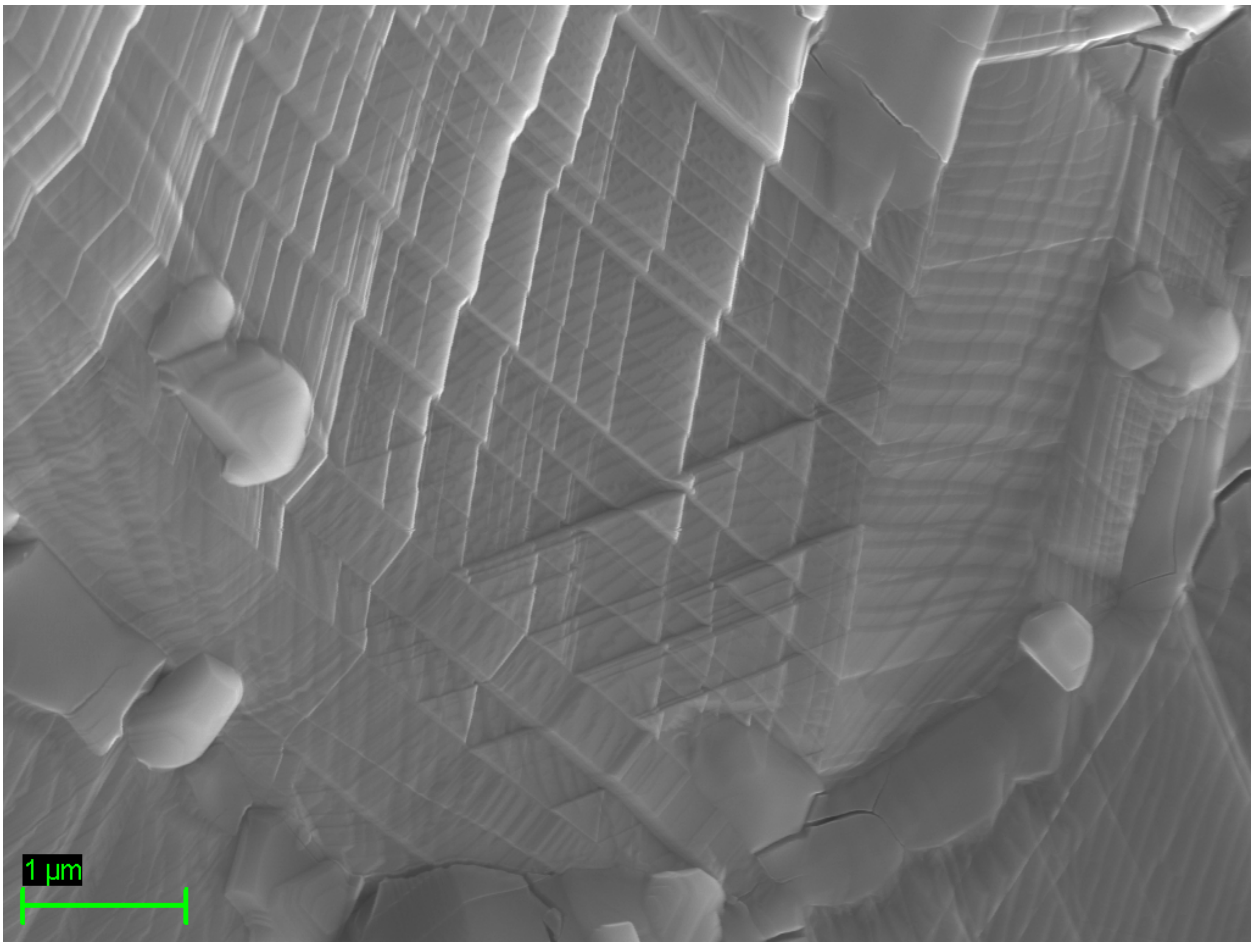

Nano-constellation- High Entropy Alloy Nanoparticles formation via Pulsed- laser induced dewetting

Nagarajan Anna Ramesh Babu

Scanning Electron Microscopy image of the intermediate stage to nanoparticle stage transition for a 15 nm film showing that the break-up of arms of the polygons via a Rayleigh-type process, leading to multiple nanoparticles in each arm. It was imaged using SEM FEI Quanta 600.

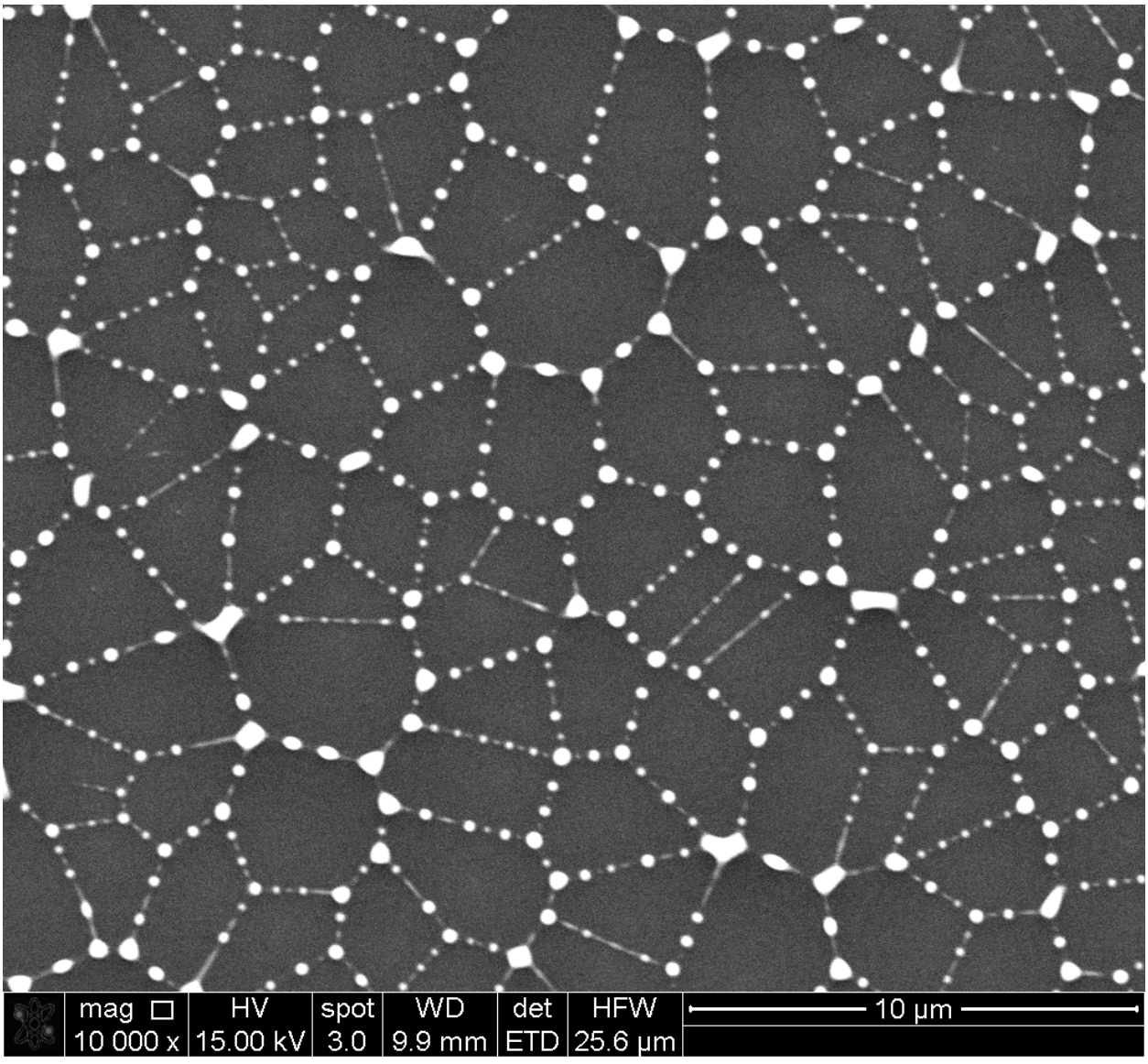

Protonic ceramic electrochemical cell - cross section

Sooraj Patel, Iman Ghamarian

This micrograph presents a cross-sectional view of a proton-conducting solid oxide electrochemical cell, captured by scanning electron microscopy using back-scattered electron imaging to reveal atomic-weight contrast. In the lower region, the porous anode displays bright NiO and dark $BaCe_{0.7}Zr_{0.1}Y_{0.1}Yb_{0.1}O_{3-\delta}$ phases. At the center lies a dense electrolyte layer, approximately 5 µm thick, composed of $BaCe_{0.4}Zr_{0.4}Y_{0.1}Yb_{0.1}O_{3-\delta}$. The upper segment consists of a porous cathode made of $BaCo_{0.4}Fe_{0.4}Zr_{0.1}Y_{0.1}O_{3-\delta}$. The layered architecture highlights the structural complexity and functional design of proton-conducting ceramic electrochemical devices.

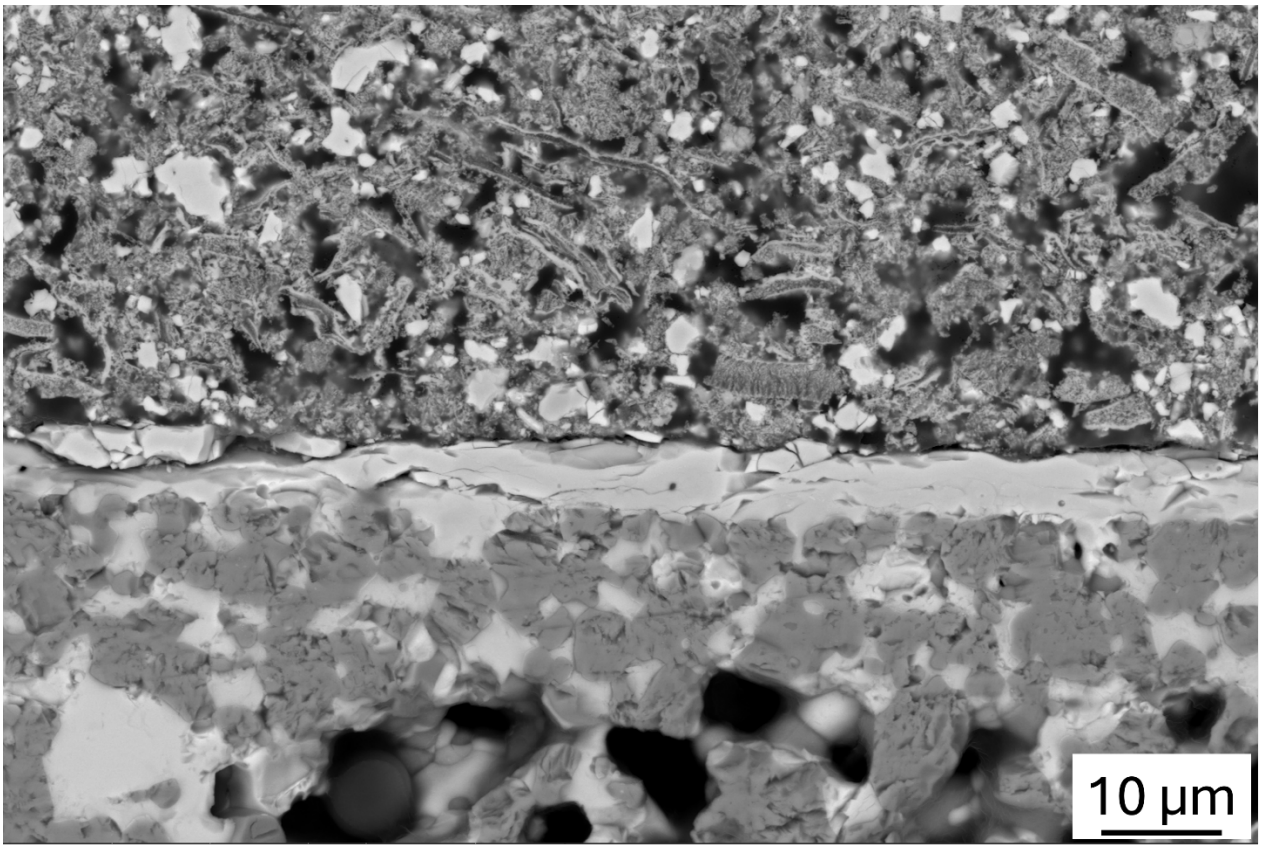

Intracellular Gold Trafficking

Mobina Mohammadnejad

Confocal laser scanning micrograph of expanded RAW 264.7 macrophages (murine macrophage cell line) treated with 100 nm gold nanoparticles. Cells were incubated with nanoparticles, fixed, quenched, expanded using the Magnify protocol, and pan-stained prior to imaging. Grayscale reveals cellular ultrastructure, while red puncta represent unlabeled gold nanoparticles detected via reflected signal. The image shows nanoparticles are localized within intracellular vesicles. Image acquired using a Zeiss LSM 780 confocal microscope. Scale bar: 50 µm.

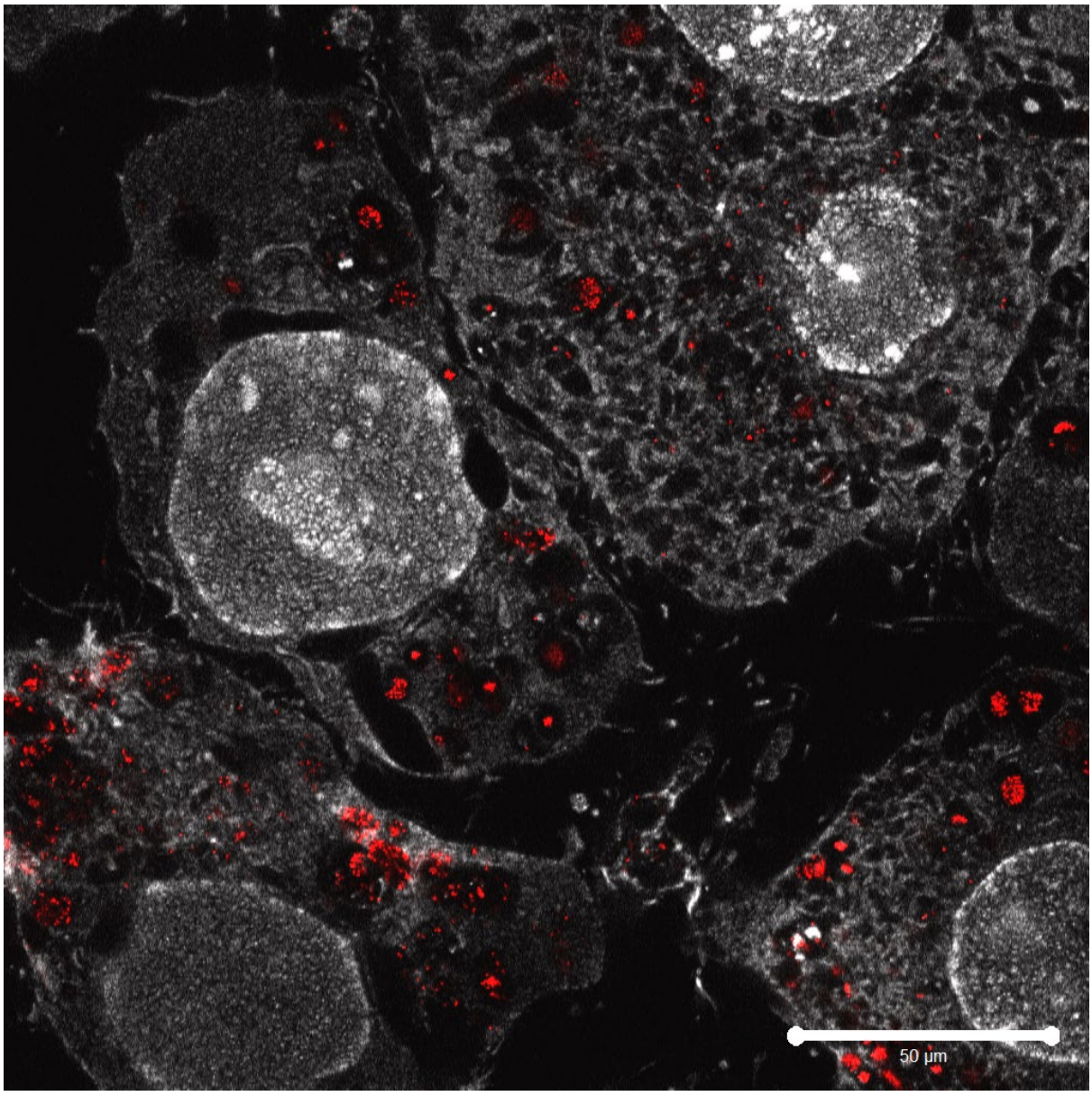

Spacecraft drifting through a cosmic void

Sagarika Das

This micrograph shows the dissected third instar larval eye of Drosophila melanogaster following co-infection with two viruses. Tissues were dissected and stained with cleaved Dcp-1 antibody (secondary A594) to detect apoptosis. The fluorescent puncta indicate apoptotic cells induced by the combined viral effects. Samples were prepared using standard immunostaining protocols and mounted for imaging. The image was acquired using a Zeiss Axio Scope microscope at 10× magnification under fluorescence conditions. The pattern of cell death highlights localized responses within the developing eye tissue.